Torque Ripple Reduction of Interior Permanent Magnet Synchronous Motor Using Harmonic Injected Current

Geun-Ho Lee[1], Sung-Il Kim[1], Jung-Pyo Hong[1], and Ji-Hyung Bahn[2]

[1]Department of Automotive Engineering, Hanyang University, Seoul 133-791, Korea
[2]Power Transformer Technology Development Team, Hyosung Co. Ltd., Changwon, Gyeongnam 641-712, Korea

Interior permanent magnet synchronous motor (IPMSM) is widely used for many industrial applications such as power train, compressor and home appliances due to its high power density and wide speed range. However, IPMSM have relatively high torque ripple in comparison with surface mounted permanent magnet motor. In case of IPMSM, d-axis current should be fed to use reluctance torque, and the more d-axis current is needed as the motor speed goes up. Therefore, back electromotive force (EMF) of IPMSM contains much harmonics and torque ripple tend to increase as the motor speed increase. This paper proposes a method to reduce torque ripple using harmonic injected current. Firstly dominant harmonic order of back EMF is investigated then under the consideration of harmonics, torque ripple using harmonic injected current will be compared with that of sinusoidal current by finite element analysis.

***Index Terms*—Finite element analysis, harmonic current injection, interior permanent magnet synchronous motor (IPMSM), torque ripple.**

I. Introduction

INTERIOR permanent magnet synchronous motor (IPMSM) has advantage of using not only magnetic torque but reluctance torque which is generated by difference of inductances between d-axis and q-axis. The IPMSM is now widely used for many industrial applications such as power train for the hybrid electric vehicle, compressor and home appliances due to its high power density and wide speed range in comparison with surface permanent magnet synchronous motor (SPMSM) [1]. Especially, in the industrial applications, there is growing interest in applying concentrated winding IPMSM to minimize the production cost and increase the productivity.

However, torque ripple in IPMSM is often a major concern in applications where speed and position accuracy is great important. In case of IPMSM, d-axis current should be fed to use reluctance torque and the more d-axis current is needed as the motor speed increase. Therefore, back electromotive force (EMF) of IPMSM contains much harmonics; hence, a ripple occurs in the output torque when driven by a sinusoidal current.

In order to minimize cogging torque and harmonics in the induced back-EMF, [2] and [3] introduce structures such as distributed winding and skewed rotor, which result in increased production cost and loss in productivity and power density.

The solution to the torque ripple is being examined in terms of the control current waveform. With such an approach, torque ripple is compensated by means of specific current waveforms using Fourier series or torque observers [4], [5].

On the other hand, some current control methods are introduced to reduce torque ripple using modified current such as deadbeat current control [6], and repetitive control technique [7].

The aim of this paper is to reduce torque ripple with harmonic injection current. Firstly numerical analysis is performed using sinusoidal current. From the result, dominant harmonic order of back-EMF is investigated, then under the consideration of distorted back EMF, torque ripple using harmonic current injection is compared with that of sinusoidal current by finite element analysis (FEA).

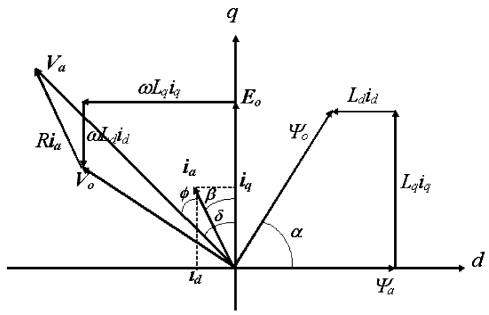

Fig. 1. Vector diagram of IPMSM.

II. Analysis Model

A. Basic Equation

Fig. 1 shows the vector diagram the IPMSM and the voltage equation in the steady state is expressed in d-q coordinates as follows [1]:

$$\begin{bmatrix} V_d \\ V_q \end{bmatrix} = \begin{bmatrix} R_a + pL_d & -\omega L_q \\ \omega L_d & R_a + pL_q \end{bmatrix} \begin{bmatrix} I_d \\ I_q \end{bmatrix} + \omega \begin{bmatrix} 0 \\ \psi_a \end{bmatrix} \tag{1}$$

and torque equation is given by

$$\begin{aligned} T &= P_n\{\psi_a i_q + (L_d - L_q) i_d i_q\} \\ &= P_n \left\{ \psi_a i_a \cos\beta + \frac{1}{2}(L_q - L_d) i_a^2 \sin 2\beta \right\} \\ &= T_m + T_r \end{aligned} \tag{2}$$

where i_d, i_q: d- and q-axis components of armature current; V_d, V_q: d- and q-axis component of armature voltage; ψ_a: flux

Digital Object Identifier 10.1109/TMAG.2008.915776

Color versions of one or more of the figures in this paper are available online at http://ieeexplore.ieee.org.

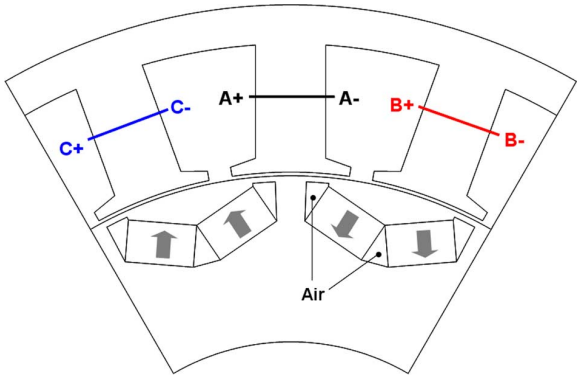

Fig. 2. Analysis model.

TABLE I
THE SPECIFICATIONS OF ANALYSIS MODEL

Parameter		Value	Unit
Pole/Slot		12/18	
Stator diameter		292	mm
Rotor diameter		204.8	mm
Stack length		85	mm
Air-gap		0.9	mm
Number of turn per phase		144	turn
Permanent magnet	Remanent flux density	1.24	T
	Relative permeability	1.05	
Dc link voltage		320	V
Rated output power		20	kW
Rated current		70	A_{rms}
Core material		RM14	
Phase resistance		103.8	mΩ

linkage due to permanent magnet; L_d, L_q: inductance along d-, and q-axis; $p = d/dt$; P_n: number of pole pairs; β: lead angle of current vector from q-axis; I_a: armature current in d-q coordinates.

The first term of right side in torque equation is the magnetic torque which is generated by armature current and permanent magnet and second term is reluctance torque component which is generated by the difference of inductances between d-q axes.

B. Analysis Model

The analysis model is designed for traction motor of hybrid electric vehicle. Rated power of the analysis model is 20 kW and its maximum output torque is 280 Nm at 680 rpm. Base speed is 680 rpm and constant power speed range (CPSR) is from 680 rpm to 3400 rpm. Fig. 2 shows the configuration of the IPMSM with concentrated winding. The specification of the analysis model is listed in Table I.

C. Torque Ripple

Fig. 3(a) and (b) indicates generated torque of the analysis model by a sinusoidal current at the base speed and the maximum speed respectively. At the base speed, the torque is obtained when current is 68 Arms and β is 48°. And maximum speed torque is calculated by 65 Arms when β is 81°. Each result is obtained by 2D-FEA.

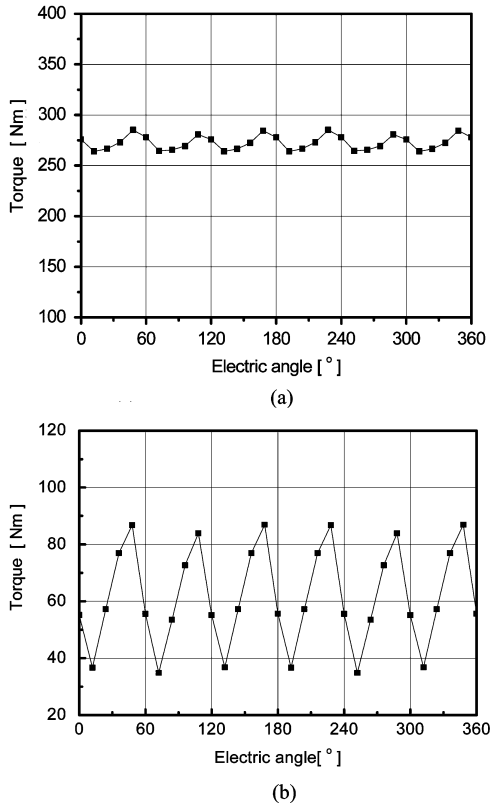

Fig. 3. Torque profile at the base speed and the maximum speed (a) Generated torque at 680 rpm and (b) generated torque at 3400 rpm.

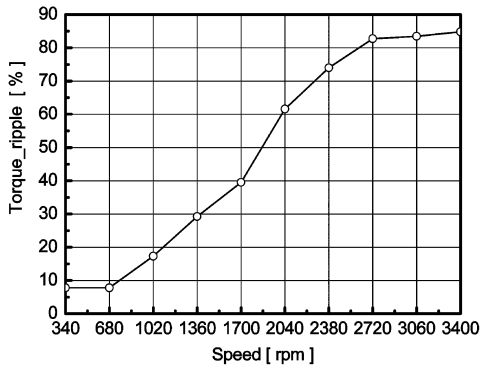

Fig. 4. Variation of torque ripple according to speed.

As shown in Fig. 3, average torque is 272.6 Nm and torque ripple is 7.8% at the base speed but at the same time average torque at the maximum speed is 61.6 Nm and torque ripple is 84.6%. Torque ripple at base speed is not a significant concern. However, torque ripple at the maximum speed can be a problem in a system which needs accurate position and speed control. Fig. 4 is the variation of torque ripple according to the speed. It is possible to say that torque ripple in the IPMSM tend to increase when flux weakening control is applied.

III. HARMONIC INJECTED CURRENT

A. Harmonic Analysis of Flux Linkage

Fig. 5 shows flux linkage at no-load and the maximum speed obtained by 2D-FEA. Fig. 6(a) and (b) shows the harmonic anal-

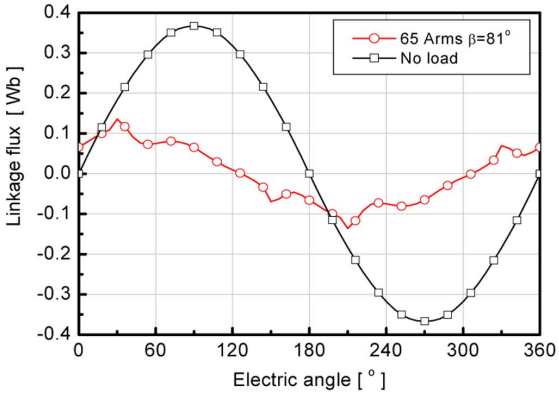

Fig. 5. Flux linkage at no-load and maximum speed.

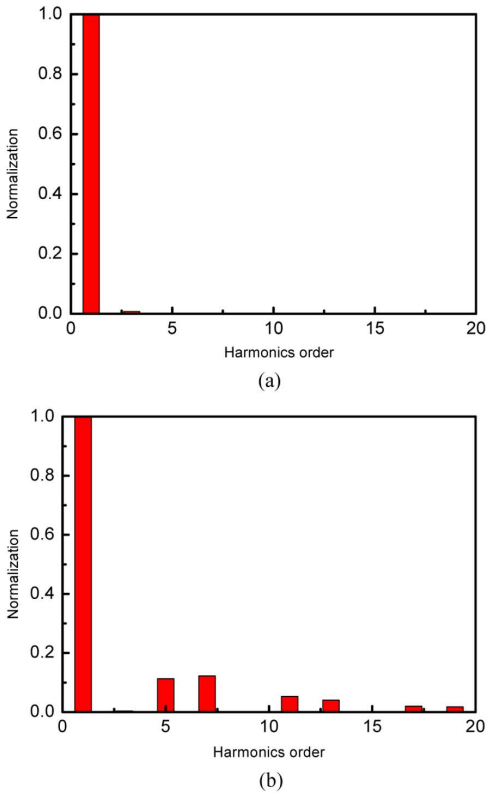

Fig. 6. Harmonic analysis of flux linkage. (a) @ No-load (b) @ Maximum speed.

ysis results of each flux linkage using discrete Fourier transform (DFT) respectively. As it can be seen, no load flux linkage has little harmonics and its total harmonic distortion (THD) is 0.5%. However, as shown in Fig. 6, flux linkage at the maximum speed contains much more harmonics than that of no load flux linkage. Even though the analysis model is designed to minimize the THD of no-load flux linkage, as the d-axis current is increased, THD of flux linkage at the maximum speed is increased to 18.2%.

In the harmonic analysis result, $6\mathrm{n} \pm 1$th harmonics are dominant harmonic. In this paper, consideration of 5th and 7th, harmonics, phasor diagram of flux linkage at base speed and maximum speed are indicated in Fig. 7.

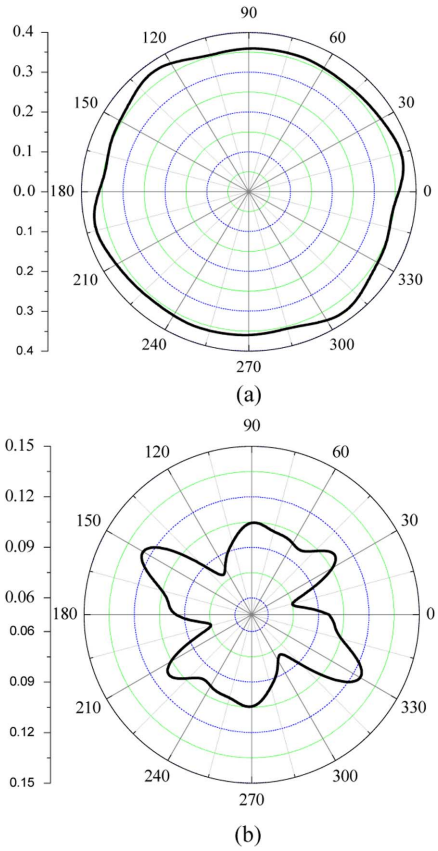

Fig. 7. Phasor diagram of flux linkage. (a) @ Base speed and (b) @ maximum speed.

B. Harmonic Injected Current

Since the torque ripple occurs when sinusoidal current interacts with the distorted back-EMF V_o, supposing that rotational speed is constant, torque ripple can be constant by using harmonic current injection. Considering the phasor diagram of the linkage flux, following current will ensure a constant torque

$$V_o \cdot I_{\mathrm{inst}} = 1 = \mathrm{const} \tag{3}$$

where V_o and I_{inst} are the instantaneous values of back-EMF and stator current respectively.

The flow chart to achieve the harmonic injected current to reduce torque ripple is shown in Fig. 8. Fig. 9 shows the harmonic injected current to achieve minimization of the torque ripple. The current is obtained by considering phasor diagram and harmonic component of the linkage flux on the assumption that the rotational speed is constant.

IV. Result

Harmonic analysis result of the harmonic injected current is indicated in Fig. 10. The result shows 5th and 7th harmonics are also dominant harmonic. As it can be seen, the rate of 5th and 7th harmonics to the fundamental is almost same with that of flux linkage.

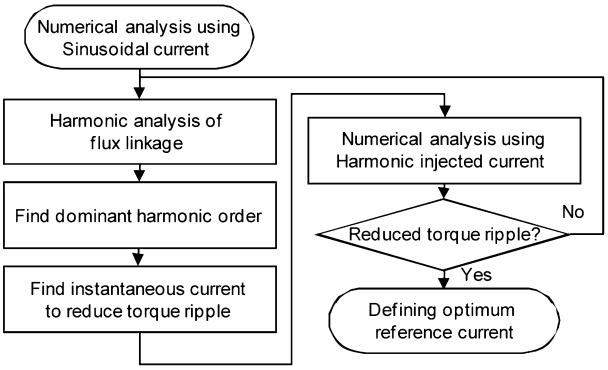

Fig. 8. Flow chart to obtain harmonic injected current.

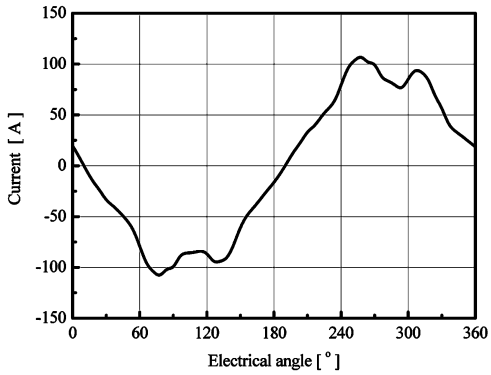

Fig. 9. Harmonic injected current.

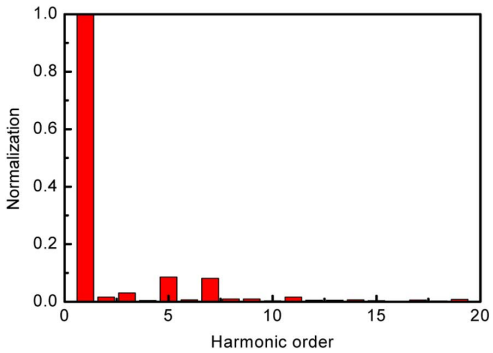

Fig. 10. Harmonic analysis of harmonic injected current.

Comparison of generated torque by sinusoidal current and harmonic injected current is shown in Fig. 11. In case of using a sinusoidal current, input current is 65 Arms. On the other, harmonic injected current is 69 Arms. Lead angle of current vector from q-axis is 81° for each model. As shown in Fig. 11, generated average torque by a sinusoidal current is 61.6 Nm and torque ripple is 84.6%. At the same time, by using harmonic injected current, average torque is increased to 74.1 Nm and torque ripple is fallen to 48.1%. By using harmonic current injection, average torque increased by 20% and torque ripple is decreased from 84.6% to 48.1%.

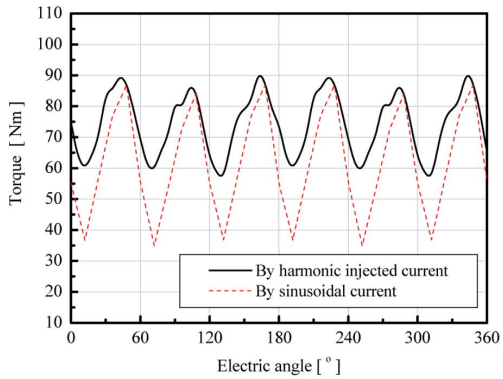

Fig. 11. Comparison of torque ripple.

V. Conclusion

In this paper, torque ripple in the IPMSM according to the rotational speed is presented. From the analysis results, it is possible to say that torque ripple of the IPMSM tends to increase when flux weakening control is applied.

This paper has proposed a method to find harmonic injected current to achieve minimization of torque ripple. Using the proposed method average torque is increased by 20% and torque ripple is decreased from 84.6% to 48.1%. This method can be used to improve the accuracy of speed and position when flux weakening control is applied.

Acknowledgment

This work was supported by the research fund of Hanyang University (HY-2006-I).

References

[1] J. Y. Lee, S. H. Lee, G. H. Lee, J. P. Hong, and J. Hur, "Determination of parameters considering magnetic nonlinearity in an interior permanent magnet synchronous motor," *IEEE Trans. Magn.*, vol. 42, pp. 1303–1306, Apr. 2006.

[2] T. Li and G. Selmon, "Reduction of cogging torque in permanent magnet motors," *IEEE Trans. Magn.*, vol. 25, pp. 2901–2903, Nov. 1988.

[3] B. Ackerman, J. H. Janssen, R. Sottek, and R. I. Van Steen, "A new method for reducing cogging torque in a class of brushless DC motors," *Proc. Inst. Elect. Eng. Elect. Power Applicat.*, vol. 139, no. 4, pp. 315–318, 1992.

[4] C. Marchand and A. Razek, "Optimal torque operation of digitally controlled permanent magnet synchronous motor drives," *Proc. Inst. Elect. Eng. B Elect. Power Applicat.*, pp. 232–240, 1993.

[5] H. Le Huy, R. Perret, and R. Feuillet, "Minimization of torque ripple in brushless DC motor drives," *IEEE Trans. Ind. Appl.*, pp. 748–755, 1986.

[6] L. Springob and J. Holtz, "High-bandwidth current control for torque ripple compensation in PM synchronous machines," *IEEE Trans. Ind. Electron.*, vol. 45, pp. 713–720, Oct. 1998.

[7] P. Mattavelli, L. Tubiana, and M. Zigliotto, "Torque-ripple reduction in PM synchronous motor drives using repetitive current control," *IEEE Trans. Power Electron.*, vol. 20, pp. 1423–1431, Nov. 2005.

Manuscript received June 24, 2007. Corresponding author: J.-P. Hong (e-mail: hongjp@hanyang.ac.kr).